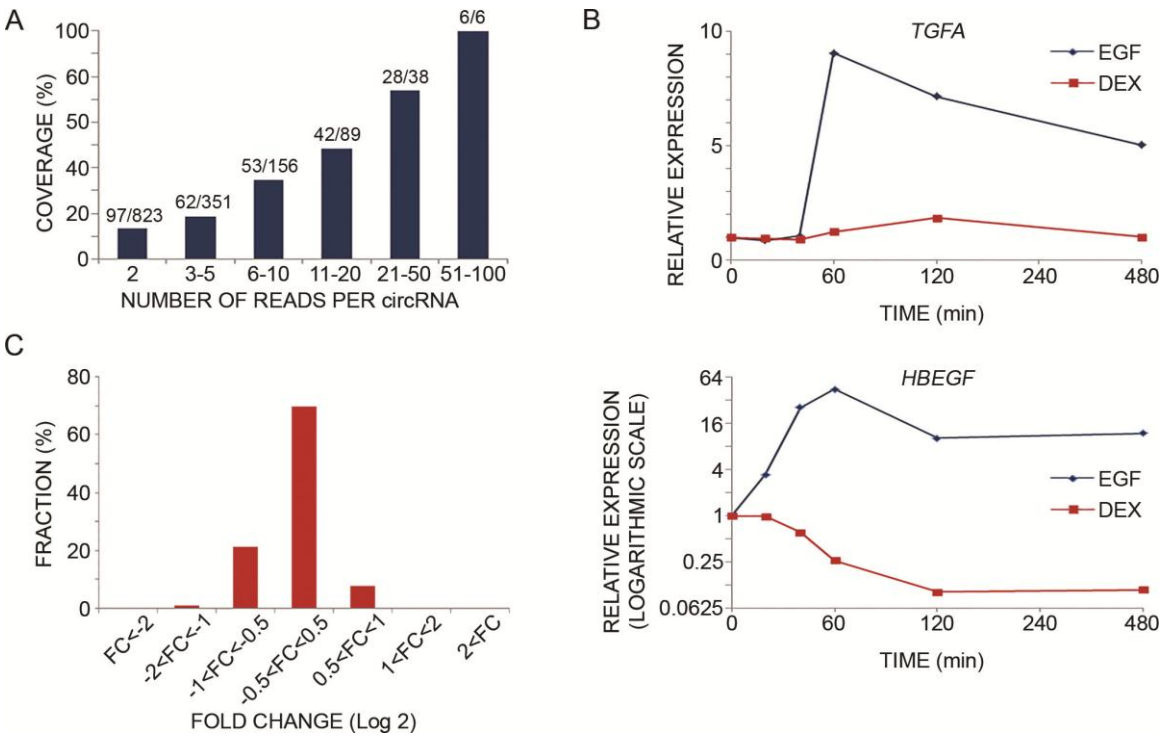

Figure S1. RNA-sequencing and time-dependent EGF-inducible expression profiles of *TGFa* and *HBEGF*. (A) A histogram presenting the distribution of RNA-Seq read numbers of circRNAs and the fraction of circRNAs measured by Fluidigm for each bin. The numbers above the bars represent the following: (number of circRNAs measured by Fluidigm) divided by (total number of candidate circRNAs). (B) MCF10A cells were treated with EGF (10 ng/ml) or DEX (100 nM) for the indicated time intervals, as described in the legend to Figure 1. High throughput PCR (Fluidigm) was used to determine abundance of mRNAs corresponding to *TGFa and HBEGF* (see Methods). (C) A histogram showing the range of abundance changes of circRNAs (N=89) displayed by EGF-stimulated MCF10A cells. To construct the histogram, the maximal change value (induction or repression) of 8h or 26h of stimulation was found for each RNA molecule.

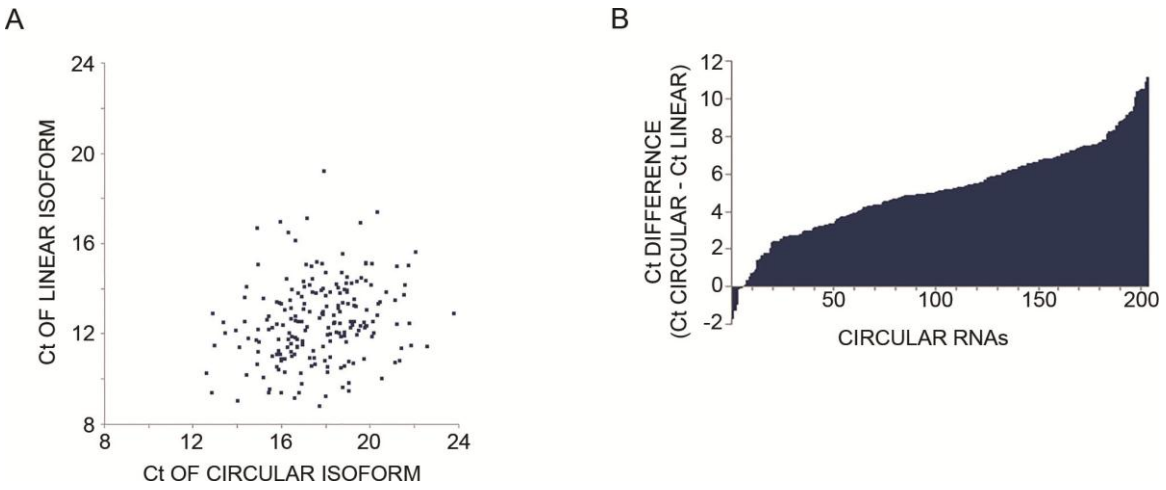

Figure S2. Relations between Ct values of circRNAs and their linear counterparts. (A) Ct values, as determined by Fluidigm, of linear RNA (N = 203) isoforms are presented against Ct values of the corresponding circular isoforms expressed in un-stimulated MCF10A human mammary cells. Pearson correlation coefficient = 0.22. (B) A histogram showing difference between Ct values of circRNAs and their corresponding linear isoforms ('Ct of circRNA' minus 'Ct of linear RNA') for 203 circRNAs expressed in MCF10A cells. Note that the vast majority of values (198 out of 203) are positive, meaning that the respective circRNAs have Ct values higher than their corresponding linear isoforms. Hence, most (>97%) circRNAs are less abundant than their corresponding linear isoforms.

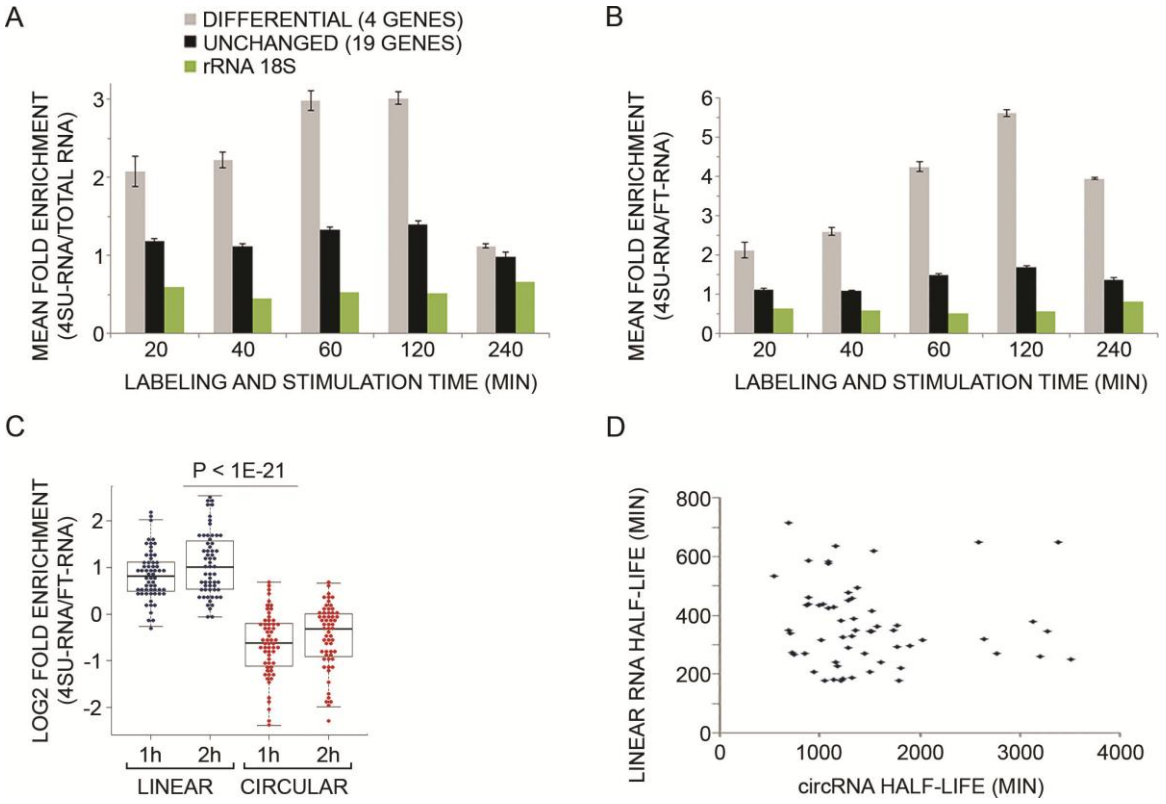

Figure S3. Newly transcribed RNA is enriched for short-lived linear RNA isoforms and displays low abundance of the respective long-lived circular isoforms. (A and B) MCF10A cells were treated with EGF for the indicated time intervals (20, 40, 60, 120 and 240 min) and simultaneously labeled with 4sU. Shown are the mean fold enrichments in 4sU labeled vs. total RNA (Y axis) (A) or flow-through RNA (B), based on Fluidigm quantification. Grey: 4 genes (*EGR1, TGFa, HBEGF* and *TXNIP*) whose expression changes in response to EGF (either induced or repressed). Black: 19 control genes whose expression does not change during the response to EGF; Green: long-lived rRNA 18S control. Error bars represent the standard error. The legend of panel A, including color codes, is shared with panel B. (C) MCF10A cells were treated with EGF for the indicated time intervals (1 and 2 h) and simultaneously labeled with 4sU. The boxplot diagram presents log2 fold enrichments for 4sU-labeled RNA relative to pre-existing (flow-through) RNA (Y axis) ($P < 1e-21$, T-test, two-tailed distribution, unequal variance, Bonferroni corrected for multiple comparisons, N=61). (D) A scatter plot displaying half-lives of linear RNAs against half-lives of the corresponding circRNAs as determined by analysis of nascent RNA. Half-lives were calculated from the ratios between nascent (RNA-4sU) and pre-existing RNAs (RNA-FT). The calculations were performed using the HALO software (Friedel et al., 2010) on RNA isolated from un-stimulated MCF10A cells labeled for 60 min with 4sU. All data were corrected for any bias due to relatively shorter RNA length. Pearson correlation coefficient = -0.06.

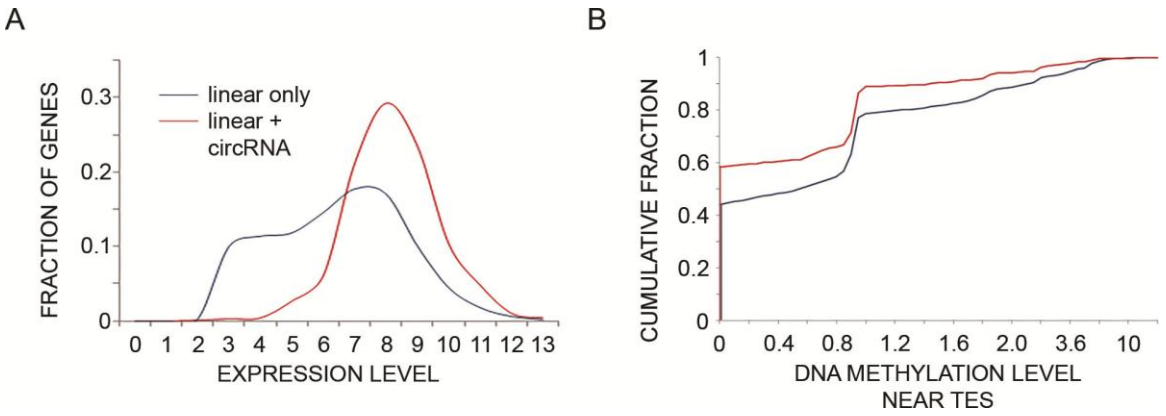

Figure S4. Genes giving rise to circRNAs also generate the respective linear RNAs and they display less DNA methylation near TES compared to genes transcribed into linear RNA only. (A) Basal (un-stimulated) expression levels of linear RNAs transcribed from genes that also give rise to circRNAs (red line; N = 975) are compared to expression levels of linear RNAs transcribed from genes that give rise only to linear RNAs (blue line; N = 16,151). Data was taken from our previously described exon microarray analyses (reference 41; P = 1e-201, T-test, two-tailed distribution, unequal variance). (B) Cumulative distribution of basal DNA methylation levels at the transcription end site (TES ± 1,000 bp) of genes transcribed into both circular and linear RNA (N = 898) is compared to the cumulative distribution of methylation displayed by genes that give rise to linear RNA only (no detectable circRNAs; N = 5,916). Note that DNA methylation levels are lower in genes producing circRNAs compared to the control group of genes (*P* = 4.79e-15, Mann-Whitney-U test).

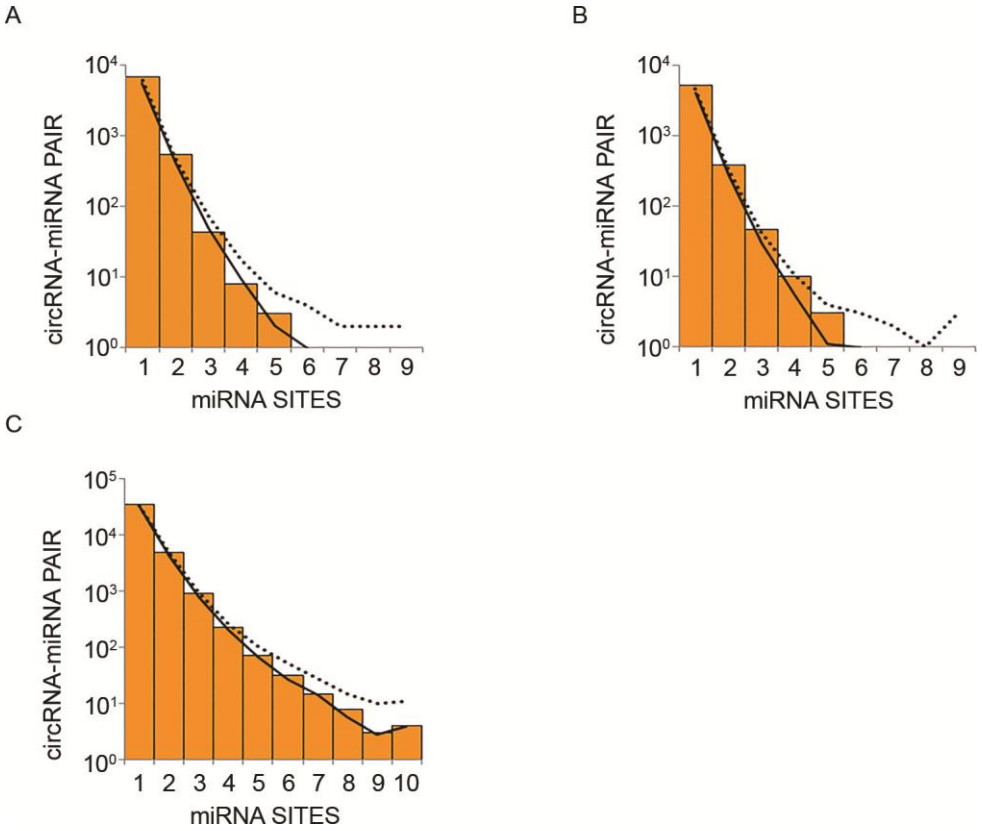

Figure S5. CircRNAs show no enrichment for potential microRNA binding sites. (A and B) Numbers of 7- and 8- nucleotide long sites for individual miRNA families found within each circRNA. The number of sites was tallied for each circRNA-miRNA pair, and the distribution of values is plotted. The miRNAs seeds were taken from 87 miRNA families conserved across all vertebrates (A) and 66 miRNA families conserved only among mammals (B). The solid black and dotted black curves indicate the averaged and 95% upper percentile, respectively, of results when repeating the analysis 1,000 times using different permutations of the sequences corresponding to the miRNA site. (C) Numbers of 6 nucleotide long sites (taken from window of nucleotides 7-12) of each miRNA found within each circRNA. The number of sites was tallied for each circRNA-miRNA pair, and the distribution of values is plotted. The solid black and dotted black curves indicate the averaged and 95% upper percentile, respectively, of results when repeating the analysis 1,000 times using different permutations of the sequences corresponding to the miRNA site.

Table S1. Circular RNAs expressed in MCF10A human mammary cells.

	1st Round	2nd Round	3rd Round
Total number of reads	71.19×10^6	182.80×10^6	148.46×10^6
Total number of non-ribosomal reads	12.17×10^6	17.78×10^6	47.73×10^6
Total circRNA reads	1,008	1,807	5,109
Number of circRNAs	303	369	1,191
Reads per circRNA	3.32	4.89	4.28

RNA (20µg) was extracted from MCF10A cells that were either unstimulated or pre-treated for an hour with either EGF (10 ng/ml) or dexamethasone (DEX; 100 nM). A cDNA library was generated from ribosomal RNA-depleted RNA according to Illumina's RNA-seq protocol. The cDNA library was sequenced on Illumina Hiseq 2500 using a 1 x 100 bp run (Memczak et al., 2013). Sequencing reads were then combined and used for identification of circRNAs expressed in MCF10A cells. Shown is a summary of results obtained in three independent deep-sequencing experiments.

Table S2. Half-lives of circular RNAs and their linear counterparts expressed in MCF10A human mammary cells.

Gene	circular half-life (min)	standard error	linear half-life (min)	standard error
FCHO2-chr5:72370568-72373320	2972.32	336.88	240.52	31.17
PHIP-chr6:79752559-79770535	2803.68	185.32	192.34	8.24
TMEM165-chr4:56277780-56284152	2750.00	118.97	397.09	35.86
NCAPG-chr4:17816475-17816981	2494.85	173.62	392.38	24.06
C3-chr19:6702137-6702590	2722.90	250.10	707.27	72.68
COG2-chr1:230798886-230800333	2183.73	290.17	291.87	30.10
ECT2-chr3:172499952-172504364	2208.96	15.19	347.30	35.66
PCNT-chr21:47768925-47769734	2151.57	292.01	579.83	28.49
SHOC2-chr10:112723882-112745523	1569.17	96.68	188.25	29.89
AAGAB-chr15:67524151-67529158	1661.11	122.59	316.61	24.16
CDC73-chr1:193202122-193205486	1587.44	47.32	286.74	22.01
CRKL-chr22:21288066-21288532	1516.41	27.51	217.08	21.71
PLEKHM3-chr2:208841374-208842310	1407.81	103.57	214.05	18.13
MED13L-chr12:116668337-116675510	1426.36	102.77	261.20	20.22
N4BP2L2-chr13:33091993-33101669	1506.34	102.55	385.56	13.98
NARS2-chr11:78176921-78204241	1501.38	36.19	405.79	30.34
DNAJC6-chr1:65830317-65831879	1240.19	3.43	195.13	28.83
ELK4-chr1:205585605-205593019	1173.44	14.05	198.15	26.33
NUP54-chr4:77055327-77065626	1335.86	81.76	395.95	24.75

RAB3IP-chr12:70193988-70195501	1196.89	23.99	302.24	12.01
RNF111-chr15:59323002-59323901	1039.46	16.97	167.33	22.98
ZKSCAN1-chr7:99621041-99621930	1173.90	45.57	311.70	37.54
ZNF782-chr9:99579646-99589463	1153.22	60.47	295.93	31.64
DUSP16-chr12:12672795-12674397	996.71	0.63	162.28	17.50
RNF168-chr3:196210640-196215554	980.46	70.68	175.72	20.29
KIF15-chr3:44826336-44835918	1142.92	42.56	363.80	22.65
CLIP4-chr2:29356520-29368233	1078.86	47.57	303.52	48.40
RAB11FIP1-chr8:37727937-37735069	977.47	43.99	207.18	17.99
HIPK2-chr7:139415730-139416814	1109.63	5.96	349.33	38.77
NCOA3-chr20:46252654-46262380	1032.24	26.35	298.28	45.20
CPSF6-chr12:69644908-69656342	1136.70	11.30	413.73	53.19
CAPRIN1-chr11:34093272-34098189	1066.47	60.64	355.97	66.09
SH3RF1-chr4:170076630-170077830	878.67	43.70	179.37	25.82
CEP72-chr5:619104-620376	1147.62	82.60	470.16	23.83
ZNF133-chr20:18278628-18287037	943.16	44.49	268.02	34.32
FOXK2-chr17:80521229-80526077	1120.94	8.76	450.94	57.68
SPC24-chr19:11258493-11258789	1214.83	159.43	565.50	10.59
MAPK9-chr5:179688683-179707608	1100.67	16.61	499.21	57.36
ERC1-chr12:1136913-1137738	936.12	7.49	392.86	49.25
TCP11L1-chr11:33065295-33079685	871.81	65.88	341.46	38.31
SPATS2L-chr2:201283972-201284219	1059.00	62.79	558.62	26.99
NPEPPS-chr17:45695715-45696530	1039.69	9.66	540.45	59.72
LARP4B-chr10:909682-931700	888.15	69.12	401.13	54.84
SOX13-chr1:204082042-204083733	902.08	80.49	455.77	44.65
ITPKC-chr19:41242890-41243674	679.79	78.62	234.69	17.38
ESYT2-chr7:158552176-158557544	910.24	7.41	544.15	47.39
ANKH-chr5:14741935-14758707	940.15	29.27	580.91	58.08
G3BP2-chr4:76573822-76581054	620.63	10.63	291.15	23.00
ASAP2-chr2:9458652-9468040	727.30	37.34	424.77	42.82
CARD6-chr5:40852275-40854198	967.48	5.13	678.68	91.32
OSBPL10-chr3:31917924-31921322	571.69	7.41	302.10	21.79
HAUS1-chr18:43702432-43703330	648.77	64.30	381.79	0.27
USP48-chr1:22074630-22078108	751.64	61.37	489.02	4.93
RNF214-chr11:117150623-117150975	747.48	79.18	492.17	47.50
ACADM-chr1:76211490-76216231	590.96	18.22	378.99	27.43
CLEC16A-chr16:11114049-11154879	763.30	68.07	574.77	49.44
CCT3-chr1:156303337-156304709	643.79	30.48	503.68	34.06
PSMA7-chr20:60714130-60716000	585.39	18.01	497.54	17.01
SPTAN1-chr9:131377910-131380387	543.78	23.28	685.28	25.51
SDF4-chr1:1158623-1159348	445.51	15.77	682.28	38.66

RNA was isolated from un-stimulated MCF10A cells pre-labeled with 4sU for 60 and 120 min. Half-lives of the indicated circular and linear isoforms were calculated from the ratios between nascent (RNA-4sU) and pre-existing RNAs (RNA-FT). The calculations were performed using the HALO software (ref. 39). Presented are the average and standard error of half-lives obtained from the 60 and 120 min labeling intervals. The genomic coordinates correspond to the non-canonical splice site that was used to detect the circRNA.